ELAC2 Mutations Cause a Mitochondrial RNA Processing Defect Associated with Hypertrophic Cardiomyopathy

Tobias B. Haack,[1,2,12] Robert Kopajtich,[2,12] Peter Freisinger,[3,12] Thomas Wieland,[1,2] Joanna Rorbach,[4] Thomas J. Nicholls,[4] Enrico Baruffini,[5] Anett Walther,[1,2] Katharina Danhauser,[1] Franz A. Zimmermann,[6] Ralf A. Husain,[7] Jessica Schum,[2] Helen Mundy,[8] Ileana Ferrero,[5] Tim M. Strom,[1,2] Thomas Meitinger,[1,2,9,10] Robert W. Taylor,[11] Michal Minczuk,[4,*] Johannes A. Mayr,[6] and Holger Prokisch[1,2,*]

The human mitochondrial genome encodes RNA components of its own translational machinery to produce the 13 mitochondrial-encoded subunits of the respiratory chain. Nuclear-encoded gene products are essential for all processes within the organelle, including RNA processing. Transcription of the mitochondrial genome generates large polycistronic transcripts punctuated by the 22 mitochondrial (mt) tRNAs that are conventionally cleaved by the RNase P-complex and the RNase Z activity of ELAC2 at 5′ and 3′ ends, respectively. We report the identification of mutations in ELAC2 in five individuals with infantile hypertrophic cardiomyopathy and complex I deficiency. We observed accumulated mtRNA precursors in affected individuals muscle and fibroblasts. Although mature mt-tRNA, mt-mRNA, and mt-rRNA levels were not decreased in fibroblasts, the processing defect was associated with impaired mitochondrial translation. Complementation experiments in mutant cell lines restored RNA processing and a yeast model provided additional evidence for the disease-causal role of defective ELAC2, thereby linking mtRNA processing to human disease.

Introduction

Human mitochondria house the four mitochondrial respiratory chain complexes to produce ATP through oxidative phosphorylation (OXPHOS). In addition to mitochondrial mRNAs (mt-mRNAs) coding for the OXPHOS subunits, mtDNA codes for the RNA components (22 mt-tRNAs and 2 mt-rRNAs) required for mitochondrial translation. The remaining factors involved in mitochondrial protein synthesis are nuclear encoded and need to be imported into the organelle. Among these nuclear components, more than 20 are linked to heritable disorders, including mitochondrial ribosomal subunits, aminoacyl-tRNA synthetases, tRNA-modifying enzymes, translation elongation factors, and two auxiliary proteins.[1,2] Human mt-mRNAs, mt-tRNAs, and mt-rRNAs are not transcribed in their mature form but are part of large polycistronic heavy (H) strand and light (L) strand precursor transcripts generated from the 16.6 kb mitochondrial genome. Because the mitochondrial genes are frequently adjacent to or separated by only a few noncoding nucleotides (or even overlap in ATPase 8/6 and ND4L/ND4), processing of the intervening mt-tRNAs has been proposed to concomitantly produce mt-mRNAs and mt-rRNAs.[3,4] Endonucleolytic cleavage at the 5′ and 3′ termini of the tRNAs in mitochondria relies on the RNase P complex and the RNase Z activity of ELAC2, respectively. There are two human genes encoding orthologs of the bacterial RNase Z (elaC): ELAC1 (MIM 608079) and ELAC2 (elaC homolog 1 and 2). ELAC1 codes for a short form of RNase Z that is localized in the cytosol,[5] whereas ELAC2 (MIM 605367) encodes a long form of RNase Z. In contrast to the short RNase Z found in diverse organisms, ELAC2-encoded long RNase Z is restricted to eukaryotes. Alternative translation initiation of ELAC2 generates two products, of which only the longer form localizes to mitochondria.[5] In HeLa cells, ELAC2 silencing led to increased levels of 3′ end unprocessed mt-tRNA precursors.[6,7] However, no effects on mitochondrial translation or respiration have been observed.[7]

We performed exome sequencing in two unrelated individuals with infantile hypertrophic cardiomyopathy, lactic acidosis, and isolated complex I deficiency (MIM 252010) in skeletal muscle, and we discovered pathogenic mutations in ELAC2. Subsequent screening of additional OXPHOS-deficient individuals identified a homozygous

ELAC2 missense mutation in two affected siblings in a third family, for a total of four disease alleles. Fibroblasts from these individuals had elevated levels of 3′ end unprocessed mt-tRNA levels, and we observed impaired mitochondrial translation in a mutant cell line. Despite previous siRNA-knockdown studies in HeLa cells suggesting that *ELAC2* is not crucial for mitochondrial respiration and translation,[7] we show here that this protein is necessary for efficient mitochondrial protein synthesis and OXPHOS function.

Subjects and Methods

Subjects

Written informed consent was obtained from all individuals investigated or their guardians, and the ethics committee of the Technische Universität München approved the study. Genetic, biochemical, and clinical findings of individuals with *ELAC2* mutations are summarized in Table 1. Pedigrees of investigated families are shown in Figure 1A.

Individual #61525 (II-2, c.[631C>T; 1559C>T], p.[Arg211*; Thr520Ile]), a boy, was the second child of healthy, unrelated parents from Germany (family F1 in Figure 1A). An older sister is healthy; a younger brother (#57415; II-3) is similarly affected. He was born at term but reduced fetal growth was noticed during the last 4 weeks of pregnancy and his birth weight was 2,690 g. After initially normal development, a failure to thrive was noticed at the age of 4 months. A severe hypertrophic cardiomyopathy and elevated serum lactate concentrations (5.7 mmol/l, normal range [n.r.] < 2.2 mmol/l) were noticed. A metabolic workup showed slightly elevated orotic acid in urine (12.7 mmol/mol creatinine, n.r. < 2 mmol/mol creatinine) and elevated alanine and glutamine in serum. Acylcarnitine profiles in serum were unremarkable, and so was screening for lysosomal storage disorders including Pompe disease and CDG syndromes. A myocardial biopsy showed severe myocardial damage with necrosis and enlarged mitochondria with abnormal cristae in electron microscopy.

At the age of 6 months, this boy died because of acute cardiac decompensation associated with severe lactic acidosis (16 mmol/l). Post mortem mutation screening of *SCO2* (MIM 604272) and for disease mutations in the mtDNA were normal.

His younger brother, individual #57415 (family F1: II-3 in Figure 1A, c.[631C>T; 559C>T], p.[Arg211*; Thr520Ile]), was born at term after normal pregnancy with a birth weight of 3,140 g. Development was unremarkable until the age of 3 months when, similar to his brother, a mild muscular hypotonia was noted. Further clinical features were dysphagia, retarded growth, and microcephaly (<3rd percentile). ECG showed signs of left ventricular hypertrophy and paroxysmal supraventricular extrasystoles and an echocardiography revealed a left ventricular hypertrophy without outflow tract obstruction. ProBNP was increased (1,336 pg/ml, n.r. < 100 pg/ml). Neuroimaging showed mild hyperintensities in T2-weighted MRI in the pallida and the brainstem without diffusion abnormalities. EEG was normal. Brainstem evoked response audiometry demonstrated moderate central hearing impairment. He had a mild, compensated metabolic acidosis and elevated blood lactate levels (3.8–5.7 mmol/l, n.r. < 2.2 mmol/l). Plasma amino acid analysis indicated increased alanine (682 μmol/l, n.r. 165–373 μmol/l) and glutamine (789 μmol/l, n.r. 32–129 μmol/l) levels, which were normal in a repeated analysis. Urinary organic acid analysis showed elevated 2-oxoglutarate, 3-hydroxyadipinlactone, 4-hydroxyphenyllactate, and ethylmalonic acid. Orotic acid was increased (11.5 mmol/mol creatinine). Light microscopy of skeletal muscle showed unspecific myopathic features with mitochondria of increased size and abnormal cristae structure in electron microscopy. Mitochondrial functional analysis in fresh muscle showed a decreased oxidation of pyruvate/malate, pyruvate/malate/ADP, and malate/pyruvate/malonate and a deficiency of respiratory chain complex I in frozen muscle.

The boy was treated with propranolol and captopril, a fat-rich diet (60 percent of total calories) was started, and he was substituted with coenzyme Q10 (10 mg/kg body weight), riboflavin (10 mg/kg), thiamine (10 mg/kg), and L-carnitine (15 mg/kg). During the subsequent 12 months, his cardiac function stabilized and hypertrophy slightly decreased. His psychomotor development continued to progress but is still not adequate with a status of approximately 10 months by the age of 24 months.

Individual #61982 (II-5, c.[460T>C; 460T>C], p.[Phe154Leu; Phe154Leu]), a girl, was the fifth child born to first-degree cousin parents of Arabic descent (family F2 in Figure 1A). Family history was remarkable for two previous first-trimester miscarriages and two elder sibling deaths. Her brother died at 13 days of unknown cause and her sister at 3 months resulting from cardiac failure from dilation of hypertrophic cardiomyopathy. Only rudimentary investigations were performed, which showed increased plasma lactate and ammonia.

The baby was born at 36 weeks weighing only 1,300 g. She was screened with echocardiography, which was normal. At her 2 month review, she had developed cardiomyopathy and growth continued to falter. Muscle tone appeared normal and there were no dysmorphic features. Cardiac function was stabilized medically and she was transferred to a metabolic center. Plasma lactates at the time of good cardiac compensation ranged from 5.4 to 8.1 mmol/l (n.r. 0.7–2.2 mmol/l).

Metabolic screening including blood film for vacuolated lymphocytes, white cell and plasma lysosomal cardiomyopathy screen, urinary glycosaminoglycans, transferrin isoelectric focusing, urine organic acids, and acylcarnitine profile was normal. Plasma amino acids showed only raised alanine in keeping with lactic acidosis.

Parents initially refused muscle and skin biopsies. The child deteriorated severely at 11 months of age with fulminant cardiogenic shock. She developed multiorgan failure complicated by candidal sepsis and died 20 days later.

Muscle biopsy taken during her final illness showed no major histopathological changes—oxidative enzyme activities including succinate dehydrogenase and cytochrome c oxidase (COX) were normal. Modified Gomori trichrome staining did not reveal ragged-red fibers. Respiratory chain enzyme studies revealed evidence of isolated complex I deficiency (60% of lowest control value); all other complex activities were normal.

Individual #36355 (II-1, c.[1267C>T; 1267C>T], p.[Leu423Phe; Leu423Phe]), a girl, was the first child of healthy first-degree cousins from Turkey (family F3 in Figure 1A). A younger sister (#65937, II-2) is also affected. Born at term, her birth weight, length, and head circumference were on the 10th percentile. At the age of 5 months, she first presented with two short episodes of convulsion without fever. An echocardiography performed because of a cardiac murmur revealed a left ventricular hypertrophic cardiomyopathy. She had muscular hypotonia and her

Table 1. Genetic, Biochemical, and Clinical Findings in Individuals with *ELAC2* Mutations

		ELAC2 Mutations	OXPHOS Activities and RNA Processing				Mean x-Fold Accumulation of Unprocessed RNA Intermediates		Clinical Features			
ID	Sex	cDNA (NM_018127.6) and Protein (NP_060597)	RCC	% of Lowest Control	Absolute Values	Reference Range	Muscle	Fibroblasts	AO	Course	HCM	Other Features
#61525[a]	male	c.[631C>T; 1559C>T], p.[Arg211*; Thr520Ile]			NA		NA	NA	4 months	death at 6 months	yes	intrauterine growth retardation, lactic acidosis, myocardial damage and necrosis associated with acute cardiac failure
#57415[a,b]	male	c.[631C>T; 1559C>T], p.[Arg211*; Thr520Ile]	I II II+III IV	50% normal normal normal	0.07 0.29 0.46 1.07	(0.14–0.35) (0.18–0.41) (0.30–0.67) (0.91–2.24)	167	10.6	3 months	alive at 2 years, 10 months	yes	psychomotor and growth retardation, muscular hypotonia, microcephaly, dysphagia, lactic acidosis, sensorineural hearing impairment, hyperintensities in basal ganglia at age 3 months
#61982[b]	female	c.[460T>C; 460T>C], p.[Phe154Leu; Phe154Leu]	I II II+III IV	60% ND normal normal	0.062 ND 0.085 0.021	(0.104–0.268) ND (0.040–0.204) (0.014–0.034)	NA	10.5	2 months	death at 11 months	yes	intrauterine growth retardation, lactic acidosis, cardiac failure, normal muscle biopsy findings
#36355[a]	female	c.[1267C>T; 1267C>T], p.[Leu423Phe; Leu423Phe]	I II II+III IV	82% ND 100% 78%	0.14 ND 0.08 0.70	(0.17–0.56) ND (0.08–0.45) (0.90–4.70)	NA	NA	5 months	alive at 13 years	yes	mild psychomotor delay, muscular hypotonia
#65937[a]	female	c.[1267C>T; 1267C>T], p.[Leu423Phe; Leu423Phe]	I II II+III IV	86% 100% normal normal	0.12 0.18 0.32 1.61	(0.14–0.35) (0.18–0.41) (0.30–0.67) (0.91–2.24)	30	2.6	5 months	death at 4 years, 9 months	yes later DCM	psychomotor retardation, muscular hypotonia, cardiac failure, COX-deficient fibers

Mitochondrial respiratory chain complexes (RCC) in muscle: I, NADH-CoQ-oxidoreductase; II, succinate dehydrogenase; II+III, succinate cytochrome c oxidoreductase; IV/COX, cytochrome c oxidase. Enzyme activities were determined in muscle biopsies and normalized to citrate synthase (CS). Absolute values and reference ranges are given in [mU/mU CS]. Abbreviations are as follows: AO, age of onset; HCM, hypertrophic cardiomyopathy; DCM, dilated cardiomyopathy; NA, no material available; ND, not determined.
[a]These individuals are siblings.
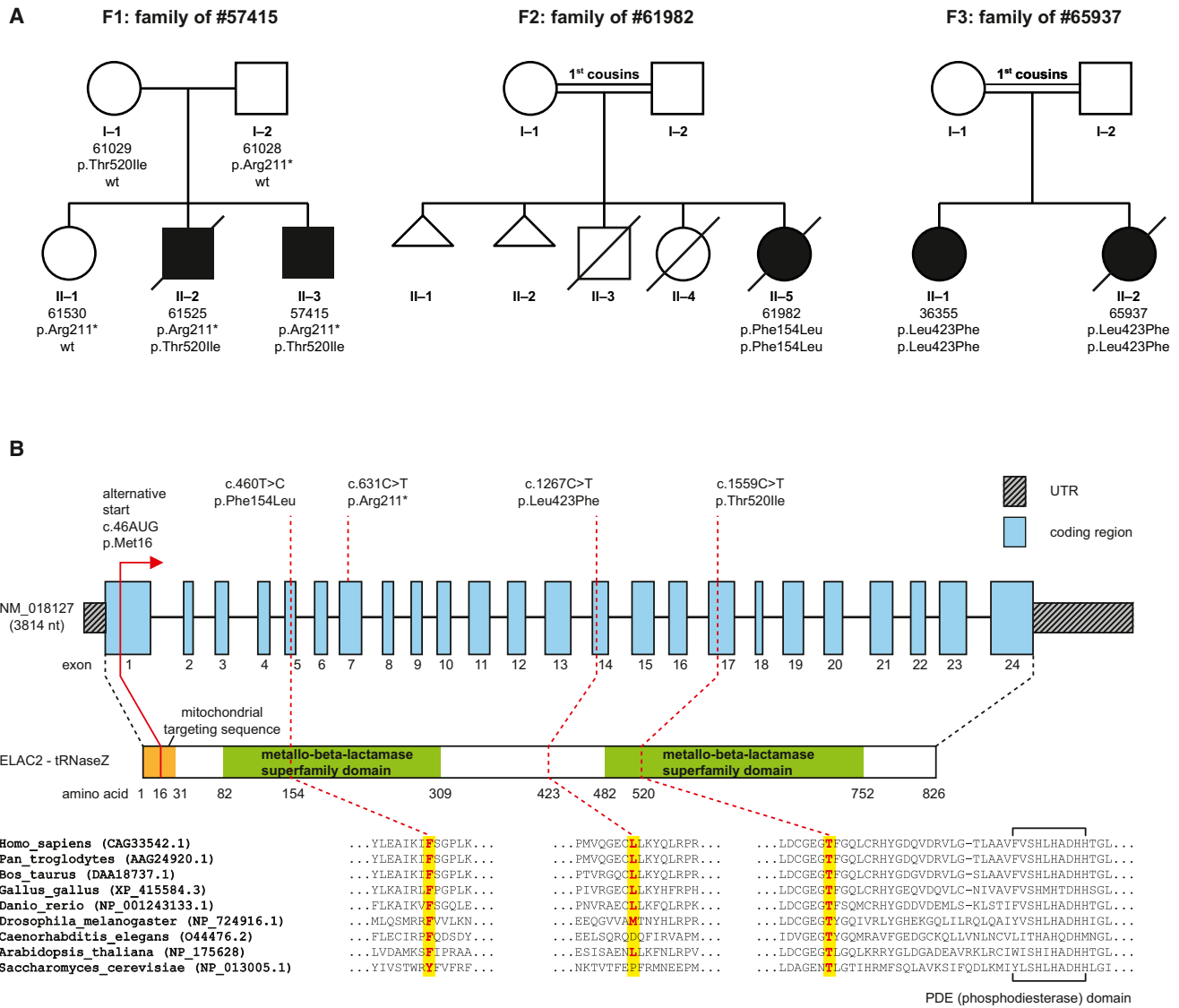[b]Investigated by exome sequencing.

Figure 1. *ELAC2* Mutation Status and Gene Structure

(A) Pedigrees of three families with mutations in *ELAC2*. Individual #57415 (F1: II-3) from unrelated parents was found to have a compound heterozygous mutation. Individuals #61982 (F2: II-5) and #65937 (F3: II-2) born to consanguineous parents (first-degree cousins) carry homozygous missense mutations in *ELAC2*.

(B) Gene structure of *ELAC2* with known protein domains of the gene product and localization and conservation of amino acid residues affected by mutations. Intronic regions are not drawn to scale.

statomotor development was delayed. Metabolic work-up was unremarkable despite slightly elevated lactate levels. Respiratory chain enzyme analysis in frozen skeletal muscle indicated reduced activities of complexes I and IV.

Over the next years a mild but constant developmental delay was documented, with sitting at the age of 18 months, first steps at the age of 24 months, and first words at the age of 30 months. A brain MRI performed at the age of 20 months was normal.

She is now 13 years old and attends a school for mentally handicapped children. The cardiac situation remained stable under a treatment with enalapril and carvedilol. The last echocardiography at the age of 13 years showed a concentric hypertrophy and a dilatation of the left ventricle (left ventricular diameter 49 mm, ventricular septum thickness 7 mm, posterior wall thickness 8 mm, fraction of shortening 22%).

The younger sister of individual #36355 (F3: II-1), subject #65937 (F3: II-2 in Figure 1A, c.[1267C>T; 1267C>T], p.[Leu423Phe; Leu423Phe]), was born at term after a normal pregnancy. At birth, her weight was 3,790 g, length 51 cm, and head circumference 36 cm, and she had an APGAR score of 9/10/10. Initial growth and psychomotor development were normal but a concentric left ventricular hypertrophy was observed at the age of 5 months. Her growth parameters were all on the 25th percentile at the age of 9 months. However, she showed muscular hypotonia, reduced head control, and a delay of motor development of approximately 5 months.

Testing of respiratory chain enzymes in a skeletal muscle biopsy taken at the age of 11 months revealed deficiencies in complexes I and IV without signs of a mitochondrial disorder in histology and histochemistry.

Her psychomotor development continued to be retarded. She started to walk at the age of 36 months and spoke two words at the age of 48 months. A treatment with furosemid, enalapril, and carvedilol failed to prevent progression of the hypertrophic cardiomyopathy to a dilated cardiomyopathy documented at the age of 4 years and 2 months together with a left ventricular fraction of shortening of 22%, a ventricular septum thickness of 8 mm, and a right bundle branch block. Clinically, she showed signs of a severe cardiac failure including arterial hypotonia (65/33 mm Hg) and renal failure resulting from reduced perfusion.

Analysis of a second skeletal muscle biopsy confirmed previous biochemical findings, but numerous COX-negative fibers were now observed.

This girl died at the age of 4 years and 9 months from cardiac failure despite intense anticongestive therapy and treatment with coenzyme Q_{10} and riboflavin.

Exome Sequencing and Variant Prioritization

We performed exome sequencing in individuals #57415 (F1: II-3) and #61982 (F2: II-5) with the SureSelect Human All Exon 50 Mb kit (Agilent) for in-solution enrichment of exonic regions followed by sequencing as 100 base-pair (bp) paired-end runs on a HiSeq2000 (Illumina).[8] For sequencing statistics see Table S1 available online. Read alignment to the human genome (UCSC Genome Browser build hg19) was done with Burrows-Wheeler Aligner (BWA, v.0.5.8) and single-nucleotide variants and small insertions and deletions were detected with BWA and SAMtools (version 0.1.7). Given that OXPHOS disorders are rare, we excluded variants with a frequency >0.2% in 1,846 control exomes and public databases. Based on a recessive model of inheritance, we next searched for genes carrying predicted homozygous or compound heterozygous nonsynonymous variants followed by a filter for genes encoding proteins with a mitochondrial localization according to a MitoP2 score > 0.5.[9]

Heteroduplex Analysis

To screen for genetic variation in ELAC2, we performed a high-resolution melting curve analysis (HRMA) in 350 individuals presenting with clinical and biochemical features suggestive of a mitochondrial disorder. Sample preparation for subsequent analysis on a LightScanner instrument (Idaho Technology) was done as described previously.[10] In brief, primers were designed to cover all 24 coding exons of ELAC2. Primer sequences and PCR protocols are available upon request. Double-strand DNA binding LCGreen Plus dye (Idaho Technology) was added to the mastermix prior to PCR. The PCR products were then covered with a layer of mineral oil before starting HRMA.

qPCR of mt-tRNAs

To verify that ELAC2 mutations impair RNase Z activity, we analyzed levels of 3′ unprocessed mt-tRNAs by qPCR. Total cellular RNA was isolated from fibroblasts of individuals #57415 (F1: II-3), #61982 (F2: II-5), and #65937 (F3: II-2) as well as from skeletal muscle of individuals #57415 and #65937. After DNase treatment (Turbo DNase, Ambion), RNA was reverse transcribed with random hexamer primers (Maxima RT, Thermo Scientific) and used for subsequent qPCR analysis. PCR reactions were set up with B-R SYBR Green SuperMix for iQ (Quanta Biosciences), covered with a layer of mineral oil, and performed in an iCycler iQ5 (BioRad Laboratories). Oligonucleotides were designed to flank RNA processing sites between tRNAs and their adjacent mRNAs or rRNAs, with one primer binding within and one primer complementary to the region downstream of the tRNA gene. Sequences of the primers used are given in Table S2. Cycle threshold (Ct) values were normalized to the mean of two housekeeping genes, HPRT1 and RPL27.

RNA-Seq of the Mitochondrial Transcriptome

The quality of the RNA isolated from whole-cell lysates was determined with the Agilent 2100 BioAnalyzer (RNA 6000 Nano Kit, Agilent). All samples had a RNA integrity number (RIN) value greater than 8. For library preparation, 1 μg of total RNA per sample was used. RNA molecules were poly(A) selected, fragmented, and reverse transcribed with the Elute, Prime, Fragment Mix (EPF, Illumina). End repair, A-tailing, adaptor ligation, and library enrichment were performed as described in the Low Throughput protocol of the TruSeq RNA Sample Prep Guide (Illumina). RNA libraries were assessed for quality and quantity with the Agilent 2100 BioAnalyzer and the Quant-iT PicoGreen dsDNA Assay Kit (Life Technologies). RNA libraries were sequenced as 100 bp paired-end runs on an Illumina HiSeq2000 platform. On average we produced about 8.4 GB of sequence per sample. With BWA (v.0.6.1) we were able to map about 75% of the reads to the human reference genome (UCSC Genome Browser build hg19). Duplicate reads were removed. For comparison, the relative coverage was calculated separately for each sample by dividing the coverage at each position by the number of reads mapped to mtDNA multiplied by 1 Mio (average number of mapped reads was 0.85 Mio over all samples).

Lentiviral Transduction

In order to prove the pathogenicity of newly identified missense alleles, we expressed the wild-type ELAC2 cDNA in fibroblasts of individuals #57415 (F1: II-3), #61982 (F2: II-5), and #65937 (F3: II-2) by using the p.Lenti6.3/V5-TOPO vector system (Invitrogen) according to the manufacturer's protocol. In brief, HEK293 FT cells cultured in 9 cm diameter dishes were cotransfected with both 600 ng pLenti6.3/V5-TOPO plasmid containing ELAC2 wild-type cDNA and 9 μg ViraPower Lentiviral Packaging Mix. After changing medium 24 hr after transfection, viruses were produced for 72 hr. Virus-containing supernatant was collected, centrifuged, diluted 1:2 in fresh medium, and used to infect the fibroblast cell lines to be transduced. At 1 day after infection, virus containing supernatant was replaced with fresh medium. At 2 days after infection, selection of transduced cells was started with blasticidin-containing medium (c = 3.6 μg/ml).[11]

Mitochondrial Translation Assays

Metabolic labeling of mitochondrial proteins with [35S]methionine was performed essentially as described previously.[2] In brief, fibroblasts derived from individual #57415 (F1: II-3) were incubated in methionine/cysteine-free medium supplemented with 2 mM L-glutamine, 48 μg/ml cysteine, 50 μg/ml uridine, and 100 μg/ml emetine dihydrochloride to block cytosolic protein synthesis. Cells were incubated for 10 min before addition of 120 μCi/ml of [35S]methionine. Labeling was performed for 30 min and the cells were washed twice with standard growth medium. Equal amounts of total cell lysates were separated by SDS-PAGE and newly synthesized proteins were quantified by autoradiography.

Immunoblotting

Supernatants from the 600 × *g* centrifugation step of tissue homogenates contain different amounts of mitochondrial proteins. Based on previous immunoblots decorated with porin antibody, the amount of crude mitochondrial extract was adjusted to yield equal amounts of mitochondrial protein by loading 4–10 μg of protein. Samples were loaded on AnykD precast gels (BioRad) and separated for 30 min at 150 V. Blotting was performed with the Trans Blot Turbo for Nitrocellulose Mini Format (BioRad) and the MixedMW transfer protocol (BioRad). Immunostaining was performed as described previously[12] with NDUFS4 (1/1,000; ab55540), SDHA (1/30,000; ab14715), UQCRC2 (1/2,000; ab14745), MTCO1 (1/1,000; ab14705), ATP5A (1/1,000; ab14748), and porin (1/1,000; ab14734) (all from Abcam) antibodies overnight at 4°C. As secondary antibody, the HRP-labeled EnVision+ Polymer anti mouse (DAKO) was diluted 1/100 and incubated for 1 hr at room temperature.

For immunoblot analysis from fibroblasts, 8 μg of total cell lysates were subjected to SDS-PAGE, transferred to nitrocellulose membrane, blocked in 5% nonfat milk in PBS for 1 hr, and incubated with specific primary antibodies overnight. The blots were further incubated with HRP-conjugated secondary antibodies for 1 hr and visualized with ECL+ (Amersham). Primary antibodies (anti-complex I subunit NDUFB8, anti-complex II subunit 30 kDa, anti-complex III subunit core 2, anti-complex IV subunit II) were purchased from Abcam.

RNA Isolation and RNA Blotting

RNA isolation and RNA blotting was performed essentially as described previously.[13] In brief, total RNA from fibroblasts of subject #57415 (F1: II-3) was isolated with Trizol (Invitrogen) according to the manufacturer's instructions. RNA was resolved on 1% agarose gels containing 0.7 M formaldehyde in 1× MOPS buffer, transferred to a nylon membrane in 2× SSC, and hybridized with either radioactively labeled PCR fragments corresponding to appropriate regions of mtDNA (to detect mt-mRNAs) or T7 RNA polymerase-transcribed radioactive RNA fragments complementary to particular mt-tRNAs. Detailed sequence information on the probes used for RNA blotting can be found in Tables S3 and S4.

Results

Exome Sequencing Identifies *ELAC2* Mutations

We performed exome sequencing to elucidate the molecular basis of the disease in individuals #57415 and #61982 (F1: II-3 and F2: II-5 in Figure 1A). Exonic regions were enriched with the SureSelect Human All Exon 50 Mb kit (Agilent) and sequenced as 100 base-pair (bp) paired-end runs on a HiSeq2000 (Illumina) to an average 110× and 152× coverage with >93% of the target being covered >20×. For sequencing statistics see Table S1.

We detected a total of ~11,000 single-nucleotide variants (SNVs) and small insertions and deletions (indels) per individual. To prioritize the likely disease-causing mutations, we applied filters accounting for the very rare and severe mitochondrial disease phenotype and an assumed recessive model of inheritance. We first excluded variants present with a frequency >0.2% in 1,846 control exomes and public databases, which left 277 (#57415, F1: II-3)

and 529 (#61982, F2: II-5) rare variants. We next searched for genes carrying either homozygous variants or two or more different heterozygous variants in the same gene and identified 9 and 67 candidates in individuals #57415 (F1: II-3) and #61982 (F2: II-5), respectively. However, in both affected individuals, only one gene, *ELAC2*, encoded a protein with a predicted mitochondrial localization (MitoP2 score > 0.5) according to the MitoP2 database.[9]

Individual #61982 (F2: II-5) carries a homozygous missense mutation, c.460T>C (p.Phe154Leu), affecting an amino acid residue conserved from human to fruit fly and worm (Figure 1B) with deleterious consequences as predicted in silico.[14,15]

Individual #57415 (F1: II-3) harbors a stop mutation, c.631C>T (p.Arg211*), compound heterozygous with a missense mutation, c.1559C>T (p.Thr520Ile), changing an amino acid conserved also in *Saccharomyces cerevisiae* with predicted pathogenic consequences. The affected sibling (#61525; F1: II-2) carries both mutations whereas the healthy parents are heterozygous carriers for one mutation each with c.631C>T being present on the maternal and c.1559C>T on the paternal allele. The healthy sister is a heterozygous carrier of the c.631C>T mutation (F1: II-1).

We next screened 350 individuals with OXPHOS disorders for genetic variation in *ELAC2* and identified a homozygous missense mutation, c.1267C>T (p.Leu423Phe), in two affected siblings (#36355 and #65937; F3: II-1 and II-2) from a third family.

Together, the identification of four different alleles (Figure 1B) in five affected individuals from three families with a similar phenotype provides strong evidence for a disease-causing role of mutant *ELAC2* in recessively inherited mitochondrial disease.

Unprocessed mtRNA Precursors Are Increased in Mutant Muscle and Fibroblasts

To directly analyze the levels of unprocessed mt-tRNAs resulting from impaired RNase Z activity in affected individual's tissues, we first used a quantitative real-time PCR (qPCR) approach. We therefore designed primers flanking ten *ELAC2* processing sites located directly upstream of mt-mRNA and mt-rRNA genes (Figure 2A). With these primers, we were able to specifically amplify unprocessed mt-tRNA-mRNA or mt-tRNA-rRNA junctions for all tRNAs tested in control muscle tissue and fibroblasts. The analysis of skeletal muscle samples available from individuals #57415 and #65937 (F1: II-3 and F3: II-2) revealed a dramatic increase in precursor levels of up to 400-fold compared to control muscle samples (Figure 2B). In contrast to skeletal muscle, the effect of the *ELAC2* mutations in fibroblasts (#57415, #61982, and #65937; F1: II-3, F2: II-5, and F3: II-2) was less pronounced, but significant with up to 30-fold increased levels of mtRNA precursors in eight out of ten processing sites in all samples (Figure 2C).

Figure 2. Quantification and Rescue of the Mitochondrial mRNA Processing Defect by qPCR

(A) Map of the mitochondrial genome with the annotation of rRNA, tRNA, and mRNA genes among the heavy and light strand. Numbering 1–10 indicates the RNA cleavage sites located 5′ terminal of rRNAs or mRNAs. As an example for the primer design, a scheme of the tRNA^{Arg}-ND4L junction is given.

(B and C) Quantification of the ten unprocessed mitochondrial tRNA-rRNA or tRNA-mRNA junctions analyzed by qPCR in (C) muscle and (D) fibroblasts before (−) and after (+) transduction with a wild-type *ELAC2* expression construct. Values are given as fold change to the average of three different controls. Error bars indicate ±1 standard deviation (SD) from the mean of at least three technical (B) or biological (C) replicates.

mt-tRNA Processing Defect Is Rescued in Mutant Fibroblasts by Exogenous *ELAC2*

In order to verify that the observed defect in 3′ end mt-tRNA processing was due to mutations in *ELAC2*, we performed cDNA complementation experiments. Lentiviral-mediated expression of *ELAC2* cDNA in fibroblasts from individuals #57415, #61982, and #65937 (F1: II-3, F2: II-5, and F3: II-2) resulted in a normalization of unprocessed mt-tRNA precursors demonstrating the rescue of the mt-tRNA processing defect (Figure 2). These results

imply that impaired RNase Z activity in mutant *ELAC2* is responsible for the mt-tRNA processing defect in all three individuals.

Mitochondrial Transcriptome in *ELAC2* Mutant Individuals

The detected processing defect suggested a possible effect on mature mt-tRNA levels. We therefore investigated the levels of 14 mt-tRNAs by RNA blotting of total RNA isolated from fibroblasts of individual #57415 (F1: II-3). We
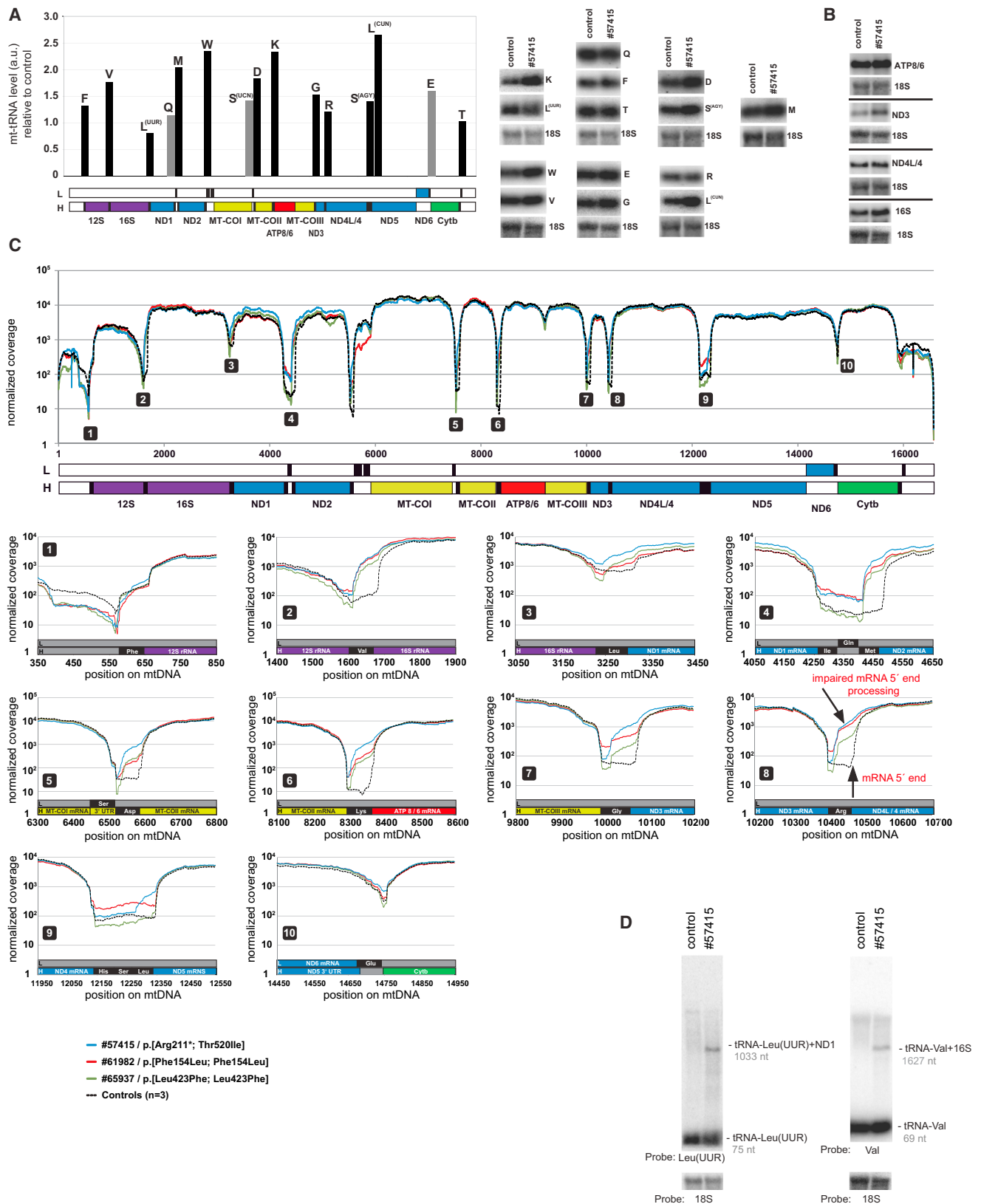
Figure 3. Steady-State Levels Mitochondrial RNAs and RNA-Seq in Mutant Fibroblasts

(A and B) Quantification of steady-state levels of (A) 14 mt-tRNAs and (B) 3 mt-mRNAs and 16S mt-rRNA in control and affected individual's (#57415) fibroblasts by RNA blot analysis. 18S rRNA was used as loading control.

(C) Mitochondrial transcriptome analysis by next-generation sequencing (RNA-seq) of fibroblasts RNA from *ELAC2* individuals and three controls. Relative sequencing coverage is plotted against the mitochondrial genome (numbering according to RefSeq accession

(legend continued on next page)

did not find a decrease in the steady-state levels in any of the mt-tRNA species investigated as compared to controls, and apparent increased levels of some mt-tRNAs were observed (Figure 3A). Additional single-nucleotide resolution RNA blots showed the mitochondrial tRNA[Leu(UUR)] and tRNA[Ser(AGY)] to be of the same length in mutant and control fibroblasts, consistent with both containing a CCA tail (Figure S1).

Because 3′ end cleavage of intervening mt-tRNAs is also crucial for the maturation of the adjacent mt-mRNAs or mt-rRNAs, we next quantified mitochondrial mRNAs and 16S-rRNA levels. However, despite the detected defect in the processing of the 3′ end of mt-tRNAs, RNA blotting did not show any considerable changes in the steady-state levels the four mtRNAs analyzed (Figure 3B).

In order to gain further insights into the properties of mtRNA of the *ELAC2* mutant individuals, we sequenced the transcriptome (RNA-seq) derived from all three individuals and three control fibroblasts. Altogether, mitochondrial transcripts represented about 4% of all sequenced transcripts. Because of their small size and the lack of poly(A) tail, mt-tRNAs were not captured for sequencing. The lack of polyadenylation in mt-rRNAs resulted in some degree of depletion of these species, so that the mt-rRNA levels obtained in the RNA-seq analysis do not represent the physiological ones. The coverage of sequenced positions of mitochondrial transcripts was on average 4,850-fold and reached 18,000-fold maximally, interspersed with regions of virtually no coverage for mt-tRNAs (Figure 3C). The number of sequence reads for each mitochondrial transcript did not vary significantly between the analyzed *ELAC2* mutant and control cell lines. This result confirms the RNA blotting data in that there were no substantial differences in the steady-state levels of both mt-rRNAs and all the mt-mRNAs between affected individual and control samples. However, the RNA-seq allowed for comprehensive analysis of processing of the 3′ and 5′ termini of all mt-mRNAs and mt-rRNAs (Figure 3C). As expected, we found no evidence of perturbed 3′ end processing of mt-mRNAs or mt-rRNAs. Also, the processing at the sites that are not punctuated by mt-tRNA (e.g., ATP8/6-MT-COIII) was not affected in the affected individual's samples as compared to the controls. However, concordant with our qPCR results, we found significantly increased amounts of 5′ end unprocessed mt-mRNA and mt-rRNA precursors at several cleavage sites that are preceded by a mt-tRNA as compared to the control cell lines (Figure 3C). The defect in the processing of mt-tRNA/mt-mRNA junctions was confirmed by RNA blotting for selected species (Figure 3D).

Together, these results suggest that impaired 3′ end processing of mt-tRNAs does not essentially reduce steady-state levels of mature mt-tRNAs or other mitochondrial transcripts, but leads to the accumulation of a substantial fraction of unprocessed mt-tRNA-RNA molecules among the mt-mRNAs.

ELAC2 Mutations Impair Mitochondrial Translation

We next tested whether the defect in mtRNA processing resulting from reduced RNase Z activity of mutant *ELAC2* affects mitochondrial translation. Fibroblasts from individual #57415 (F1: II-3) had a reduced rate of synthesis of mtDNA-encoded OXPHOS components as shown by quantification of ^{35}S-labeled methionine in the presence of emetine, an inhibitor of cytosolic translation (Figures 4A and 4B). This correlated with reduced steady-state levels of OXPHOS proteins as assayed by immunoblotting of total protein fractions from fibroblasts (Figure 4C). An impaired mitochondrial protein synthesis and/or assembly of respiratory chain complex I was also suggested by immunoblot analysis of OXPHOS levels in muscle from individual #57415 (F1: II-3), whereas complex II (which contains only nuclear encoded subunits) was found to be increased (Figure 4D). Together, these findings suggest a defect in translation of mtDNA-encoded proteins in *ELAC2* mutant tissues. These data imply a disease model whereby defective processing of precursor mtRNA exerts its effects neither via reduced levels of mature mt-tRNAs nor mt-mRNAs or mt-rRNAs but might be associated with an accumulation of processing intermediates hampering effective mitochondrial translation.

Rescue Experiments in Yeast Substantiate Pathogenicity of the Thr520Ile Mutation

To further substantiate the pathogenicity of identified *ELAC2* mutations, we studied the p.Thr520Ile substitution conserved in yeast corresponding to the change Thr513Ile in the essential RNase Z ortholog Trz1 (Figure S2A). By using the plasmid shuffling method,[16] we generated a deletion strain expressing either the *trz1* mutant or the *TRZ1* wild-type allele. In the *trz1* mutant strains, we observed a typical phenotype indicative of impaired respiratory chain function,[17] a reduced growth rate on medium containing nonfermentable carbon sources (Figure S2B). Direct testing of overall respiration rate and COX activity showed a 40% decrease in both parameters as compared to the *TRZ1* wild-type strain (Figures S2C and S2D). Assessment of mitochondrial translation by [^{35}S]methionine labeling in the presence of cycloheximide demonstrated a clear reduction in the rate of synthesis of all mtDNA-encoded gene products (Figure S2E). Furthermore, we observed a higher *petite* frequency, a finding that in yeast typically occurs when mitochondrial translation is quantitatively reduced (Figure S2F). In summary, these data confirm that the Thr520Ile

---

number J01415). Colored lines represent individuals #57415 (blue), #61982 (red), and #65937 (green). The black dotted line indicates the average of three controls. The ten RNase Z cleavage sites analyzed by qPCR (Figure 2) are shown with higher magnification.

(D) RNA blot analysis decorated with tRNA[Leu(UUR)]- and tRNA[Val]-specific probes to detect unprocessed mt-tRNA-mRNA intermediates.

A

ND5
MT-COI
ND4
ND2
CytB
ND1
MT-COII/III
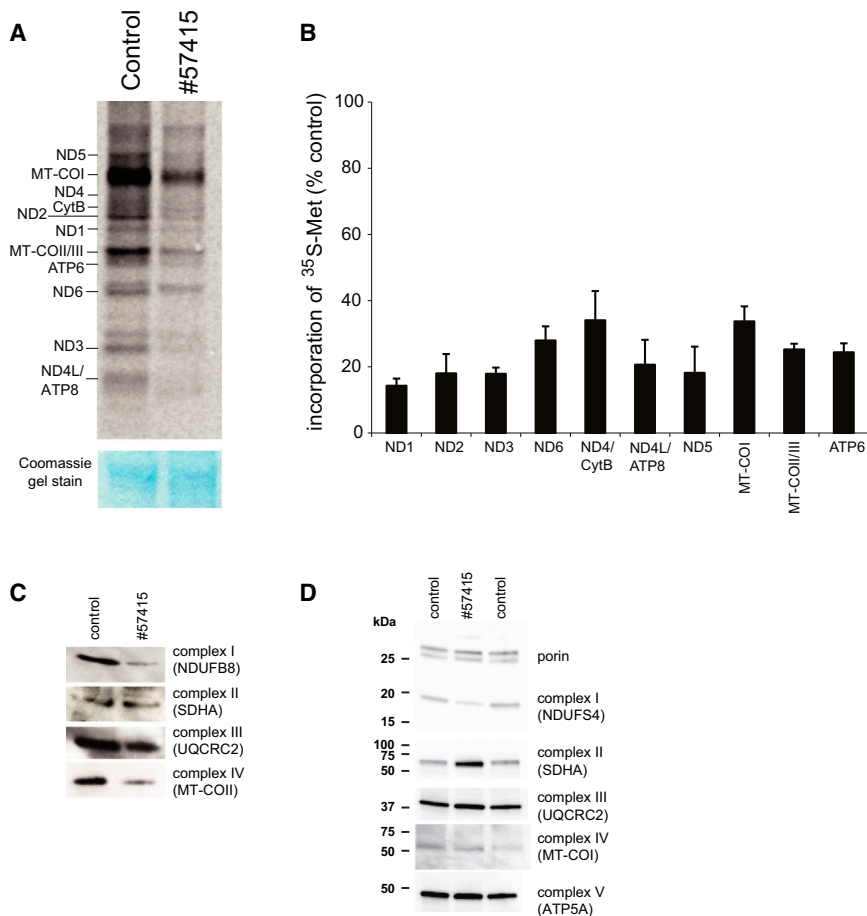ATP6
ND6
ND3
ND4L/
ATP8

Coomassie
gel stain

B

Figure 4. Mitochondrial Translation and Steady-State Levels of Respiratory Chain Complexes in Mutant Fibroblasts

(A and B) Analysis of mitochondrial translation products in fibroblasts from individual #57415 by [^{35}S]methionine pulse labeling (A) and quantification of three experiments (B). Error bars indicate ±1 SD from the mean of three replicates. mtDNA-encoded structural subunits of complex I (ND1, ND2, ND3, ND4, ND4L, ND5, ND6), complex III (cytb), complex IV (MT-COI, MT-COII, MT-COIII), and complex V (ATP6, ATP8) are shown.

(C and D) Immunoblot analysis of respiratory chain complex subunits in crude mitochondrial extractions from individual #57415 and control (C) fibroblasts as well as (D) muscle. Porin antibody was used as a loading control in muscle.

C

complex I (NDUFB8)
complex II (SDHA)
complex III (UQCRC2)
complex IV (MT-COII)

D

porin
complex I (NDUFS4)
complex II (SDHA)
complex III (UQCRC2)
complex IV (MT-COI)
complex V (ATP5A)

substitution in *ELAC2* causes defective mitochondrial respiration via impaired mitochondrial translation.

Discussion

Here, we describe five individuals with a severe, infancy-onset disorder and mutations in *ELAC2*, which has originally been reported as a susceptibility gene for heritable prostate cancer (MIM 614731). Despite a study questioning the functional consequences of cancer-associated missense variants,[18] two of them, p.Ser217Leu and p.Ala541Thr, have been reinforced as low-penetrance susceptibility markers of prostate cancer by a recent meta-analysis.[19] Alongside a potential role in tumorgenesis, ELAC2 has been shown to interact with gamma-tubulin complexes in the cytoplasm[20] and the RNAi knockdown of the *Caenorhabditis elegans* ortholog to interfere with germline proliferation.[21] Impaired mt-tRNA (or nuclear tRNA) processing may also contribute to the pathogenesis of prostate cancer; however, here we demonstrate that impaired RNase Z activity of ELAC2 causes a fatal failure in cellular energy metabolism.

OXPHOS disorders usually present with vast allelic heterogeneity and a broad spectrum of clinical manifestations, hindering attempts to establish clear genotype-phenotype correlations. Although the severity and course of the disease differs among the five *ELAC2* mutant individuals, it is important to highlight several consistent features.

Hypertrophic cardiomyopathy is a potentially life-limiting key clinical feature and has been documented in all individuals before the age of 6 months. Two genetically confirmed cases bearing the alterations p.[Arg211*; Thr520Ile] (#61525; F1: II-2) and p.[Phe154Leu; Phe154Leu] (#61982; F2: II-5) died within the first year of life due to cardiac failure, and another two siblings of #61982 (F2: II-5) with unclear genetic status but suggestive clinical presentations died before the age of 3 months. In individuals with the substitution p.[Leu423Phe; Leu423Phe] (#36355 and #65937; F3: II-1 and II-2), despite intense anticongestive therapy, cardiomyopathy progressed toward a dilated form by the age of 4 years, leading to death in one of them within 1 year. In four out of five affected individuals, a mild to marked developmental delay has been documented.

Neuroimaging studies documented hyperintensities in T2-weighted MRI in the pallida in one individual with the substitutions p.[Arg211*; Thr520Ile] (#57415; F1: II-3); another individual, #36355 (F3: II-1), had normal scans. Laboratory investigations consistently showed elevated lactate levels in blood together with associated elevations of amino acids (alanine, glutamine) in serum. Analysis of mitochondrial respiratory chain enzymes from muscle revealed a complex I defect in all affected individuals, suggesting that complex I deficiency might be the most sensitive indicator for mitochondrial dysfunction. However, the defect was mild in some and associated with a complex IV deficiency in individual #36355 (F3: II-1). In addition, numerous COX-deficient fibers were detected in case #65937 (F3: II-2) although not in all affected individuals.
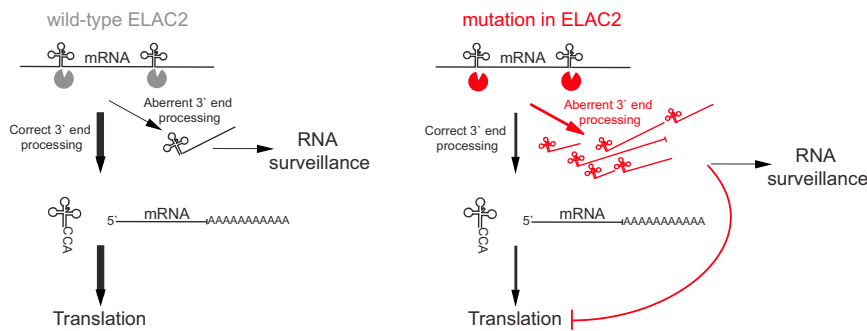
Figure 5. Model of Potential *ELAC2* Pathomechanism
Suggested model of normal and impaired ELAC2 activity. Under normal conditions minor amounts of unprocessed ELAC2 substrates can be degraded by the RNA surveillance machinery. Reduced ELAC2 activity results in an accumulation of mitochondrial precursor mRNAs, which impair mitochondrial translation.

We provide several lines of evidence arguing for a disease-causing role of *ELAC2* mutations including (1) statistical evidence by identifying four disease alleles in three families with a similar biochemical and clinical phenotype, (2) functional evidence by documentation of elevated 3′ end unprocessed tRNA levels in tissues of affected individuals that were corrected upon lentiviral expression of wild-type *ELAC2* cDNA, and (3) confirmation of the deleterious consequences of the missense mutation Thr520Ile by modeling in yeast. So far only mtDNA mutations have been implicated in tRNA processing defects.[22] The present study establishes nuclear mutations as a cause of a human disease affecting mitochondrial RNA processing.

A role of ELAC2 in mt-tRNA processing has been determined previously and was now confirmed by our study. The analysis of respiratory chain complex activities in mutant skeletal muscle demonstrated a significant OXPHOS defect, which resulted in a severe, infancy-onset disorder. Our experiments in fibroblast cell lines derived from affected individuals indicate that ELAC2 is crucial for efficient synthesis of mtDNA-encoded proteins and proper steady-state levels of structural OXPHOS components, consistent with respiratory chain defects detected in affected individual's skeletal muscle. Proper function of ELAC2 is more important in skeletal muscle than in fibroblast cell cultures, probably reflecting different needs and thresholds for mitochondrial expression of respiratory chain complexes.[23] A previous *ELAC2* RNAi knockdown study in HeLa cells suggested that mitochondrial translation and OXPHOS activity remained unaffected.[7] These divergent results may be explained by the difference of transient or persistent ELAC2 inactivation. Although RNAi can sufficiently reduce ELAC2 and leads to accumulated mtRNA precursors at the time of subsequent analyses, the exposure to these changes might be too short to manifest downstream effects, e.g., impaired mitochondrial translation. Another variable is the difference in the cell types analyzed, highlighting the importance of establishing cell lines from affected individuals, which are valuable resources for the functional work-up in metabolic disorders.

What are the mechanisms connecting impaired mitochondrial processing and altered mitochondrial translation? Mutations in several mt-tRNAs have been shown to hamper 3′ end processing and to cause defective mitochondrial respiration.[22,24,25] For example, a number of disease-linked mutations in the mt-tRNA(Leu^{UUR}) gene (e.g., m.3243A>G, m.3271T>C, and m.3302A>G) show reduced steady-state levels of this mt-tRNA in vivo, associated with an increase in corresponding precursors.[26] Further in vitro experiments demonstrated that these base substitutions in mt-tRNA(Leu^{UUR}) interfere with 3′ end processing.[27] Also, pathological mutations in the T-loop of mt-tRNA(Ile) and mt-tRNA(Gly) (m.4317A>G and m.10044A>G, respectively) result in impaired binding of substrate mt-tRNA to the 3′ processing enzyme and inhibition of CCA addition to the respective tRNA by the human mitochondrial CCA-adding enzyme.[25,28] In these cases, the mt-tRNA levels or aminoacylation became the limiting factor for mitochondrial protein synthesis. However, in contrast to prior studies suggesting decreased levels of mature mt-tRNAs upon *ELAC2* silencing, our investigations demonstrate normal levels of mt-tRNAs and no defect in maturation. Our results argue against decreased mt-tRNA levels as the limiting factor for translation resulting from impaired ELAC2 function and shifted our focus to investigate mt-mRNA processing. The concomitant maturation of mt-mRNAs by 3′ end mt-tRNA processing is a key issue, because mammalian mitochondrial 55S ribosomes preferentially form initiation complexes at a 5′-terminal AUG over an internal AUG, and it is questionable whether unprocessed mt-mRNA can be translated at all.[29] The latter finding suggests that unprocessed precursor mt-mRNAs are not efficiently translated. Based on the 400-fold increase in 5′ end unprocessed mt-mRNAs in affected individuals muscle tissue, the most direct explanation for an OXPHOS defect would be diminished levels of mature mt-mRNAs (Figure 5, in black). However, our results from RNA-seq experiments argue that a maximum of 10% of the mt-mRNAs are unprocessed at the 5′ end in mutant fibroblasts and such a minor fraction should be tolerated by the cell. Because of the limited availability of muscle tissue from affected individuals, we could not determine the ratio of processed to unprocessed mt-tRNA-mRNA junctions. The near 400-fold increase in the levels of mtRNA precursors observed in affected individuals muscle samples (compared to controls) could be considered sufficient to decrease the proportion of functional mt-mRNA molecules to the extent that translation

is significantly impaired. Nonetheless, the observed defect in mutant fibroblasts, despite practically normal levels of matured mt-tRNA, mt-mRNA, and mt-rRNA, led us to propose an additional model in which the accumulation of aberrantly processed mtRNA species that fail to be eliminated by the RNA surveillance machinery might interfere with translation (Figure 5, in red).

In conclusion, we have used exome sequencing to identify *ELAC2* mutations as the molecular genetic correlate of OXPHOS deficiency associated with infantile-onset hypertrophic cardiomyopathy, encephalopathy, and lactic acidosis. In line with an RNase Z function of ELAC2 in mitochondria, we have shown that mitochondrial RNA precursors accumulate in affected individuals fibroblasts and skeletal muscle. We established in *ELAC2* mutant cell lines and yeast that *ELAC2* and its yeast ortholog TRZ1 are crucial for efficient mitochondrial translation and function. This study highlights an important role for next-generation sequencing approaches in the investigative diagnostic algorithm for individuals with suspected mitochondrial disease because they not only reliably identify known disease mutations and genes but can also reveal fundamental insights into the underlying cell biology and pathomechanisms.

Supplemental Data

Supplemental Data include two figures and four tables and can be found with this article online at http://www.cell.com/AJHG/.

Web Resources

The URLs for data presented herein are as follows:

MitoP2, http://www.mitop.de
MutationTaster, http://www.mutationtaster.org/
Online Mendelian Inheritance in Man (OMIM), http://www.omim.org/
PolyPhen-2, http://www.genetics.bwh.harvard.edu/pph2/
RefSeq, http://www.ncbi.nlm.nih.gov/RefSeq
UCSC Genome Browser, http://genome.ucsc.edu

References

1. Pearce, S., Nezich, C.L., and Spinazzola, A. (2013). Mitochondrial diseases: translation matters. Mol. Cell. Neurosci. *55*, 1–12.
2. Rorbach, J., Gammage, P.A., and Minczuk, M. (2012). C7orf30 is necessary for biogenesis of the large subunit of the mitochondrial ribosome. Nucleic Acids Res. *40*, 4097–4109.
3. Anderson, S., Bankier, A.T., Barrell, B.G., de Bruijn, M.H., Coulson, A.R., Drouin, J., Eperon, I.C., Nierlich, D.P., Roe, B.A., Sanger, F., et al. (1981). Sequence and organization of the human mitochondrial genome. Nature *290*, 457–465.
4. Ojala, D., Montoya, J., and Attardi, G. (1981). tRNA punctuation model of RNA processing in human mitochondria. Nature *290*, 470–474.
5. Rossmanith, W. (2011). Localization of human RNase Z isoforms: dual nuclear/mitochondrial targeting of the ELAC2 gene product by alternative translation initiation. PLoS ONE *6*, e19152.
6. Brzezniak, L.K., Bijata, M., Szczesny, R.J., and Stepien, P.P. (2011). Involvement of human ELAC2 gene product in 3′ end processing of mitochondrial tRNAs. RNA Biol. *8*, 616–626.
7. Sanchez, M.I., Mercer, T.R., Davies, S.M., Shearwood, A.M., Nygård, K.K., Richman, T.R., Mattick, J.S., Rackham, O., and Filipovska, A. (2011). RNA processing in human mitochondria. Cell Cycle *10*, 2904–2916.
8. Haack, T.B., Haberberger, B., Frisch, E.M., Wieland, T., Iuso, A., Gorza, M., Strecker, V., Graf, E., Mayr, J.A., Herberg, U., et al. (2012). Molecular diagnosis in mitochondrial complex I deficiency using exome sequencing. J. Med. Genet. *49*, 277–283.
9. Elstner, M., Andreoli, C., Ahting, U., Tetko, I., Klopstock, T., Meitinger, T., and Prokisch, H. (2008). MitoP2: an integrative tool for the analysis of the mitochondrial proteome. Mol. Biotechnol. *40*, 306–315.
10. Haack, T.B., Madignier, F., Herzer, M., Lamantea, E., Danhauser, K., Invernizzi, F., Koch, J., Freitag, M., Drost, R., Hillier, I., et al. (2012). Mutation screening of 75 candidate genes in 152 complex I deficiency cases identifies pathogenic variants in 16 genes including NDUFB9. J. Med. Genet. *49*, 83–89.
11. Danhauser, K., Iuso, A., Haack, T.B., Freisinger, P., Brockmann, K., Mayr, J.A., Meitinger, T., and Prokisch, H. (2011). Cellular rescue-assay aids verification of causative DNA-variants in mitochondrial complex I deficiency. Mol. Genet. Metab. *103*, 161–166.
12. Feichtinger, R.G., Zimmermann, F., Mayr, J.A., Neureiter, D., Hauser-Kronberger, C., Schilling, F.H., Jones, N., Sperl, W., and Kofler, B. (2010). Low aerobic mitochondrial energy metabolism in poorly- or undifferentiated neuroblastoma. BMC Cancer *10*, 149.
13. Rorbach, J., Nicholls, T.J., and Minczuk, M. (2011). PDE12 removes mitochondrial RNA poly(A) tails and controls translation in human mitochondria. Nucleic Acids Res. *39*, 7750–7763.
14. Adzhubei, I.A., Schmidt, S., Peshkin, L., Ramensky, V.E., Gerasimova, A., Bork, P., Kondrashov, A.S., and Sunyaev, S.R. (2010). A method and server for predicting damaging missense mutations. Nat. Methods *7*, 248–249.
15. Schwarz, J.M., Rödelsperger, C., Schuelke, M., and Seelow, D. (2010). MutationTaster evaluates disease-causing potential of sequence alterations. Nat. Methods *7*, 575–576.
16. Baruffini, E., Ferrero, I., and Foury, F. (2010). In vivo analysis of mtDNA replication defects in yeast. Methods *51*, 426–436.

17. Ghezzi, D., Baruffini, E., Haack, T.B., Invernizzi, F., Melchionda, L., Dallabona, C., Strom, T.M., Parini, R., Burlina, A.B., Meitinger, T., et al. (2012). Mutations of the mitochondrial-tRNA modifier MTO1 cause hypertrophic cardiomyopathy and lactic acidosis. Am. J. Hum. Genet. *90*, 1079–1087.

18. Minagawa, A., Takaku, H., Takagi, M., and Nashimoto, M. (2005). The missense mutations in the candidate prostate cancer gene ELAC2 do not alter enzymatic properties of its product. Cancer Lett. *222*, 211–215.

19. Xu, B., Tong, N., Li, J.M., Zhang, Z.D., and Wu, H.F. (2010). ELAC2 polymorphisms and prostate cancer risk: a meta-analysis based on 18 case-control studies. Prostate Cancer Prostatic Dis. *13*, 270–277.

20. Korver, W., Guevara, C., Chen, Y., Neuteboom, S., Bookstein, R., Tavtigian, S., and Lees, E. (2003). The product of the candidate prostate cancer susceptibility gene ELAC2 interacts with the gamma-tubulin complex. Int. J. Cancer *104*, 283–288.

21. Smith, M.M., and Levitan, D.J. (2004). The *Caenorhabditis elegans* homolog of the putative prostate cancer susceptibility gene ELAC2, hoe-1, plays a role in germline proliferation. Dev. Biol. *266*, 151–160.

22. Bindoff, L.A., Howell, N., Poulton, J., McCullough, D.A., Morten, K.J., Lightowlers, R.N., Turnbull, D.M., and Weber, K. (1993). Abnormal RNA processing associated with a novel tRNA mutation in mitochondrial DNA. A potential disease mechanism. J. Biol. Chem. *268*, 19559–19564.

23. Mineri, R., Pavelka, N., Fernandez-Vizarra, E., Ricciardi-Castagnoli, P., Zeviani, M., and Tiranti, V. (2009). How do human cells react to the absence of mitochondrial DNA? PLoS ONE *4*, e5713.

24. Levinger, L., Mörl, M., and Florentz, C. (2004). Mitochondrial tRNA 3′ end metabolism and human disease. Nucleic Acids Res. *32*, 5430–5441.

25. Levinger, L., and Serjanov, D. (2012). Pathogenesis-related mutations in the T-loops of human mitochondrial tRNAs affect 3′ end processing and tRNA structure. RNA Biol. *9*, 283–291.

26. King, M.P., Koga, Y., Davidson, M., and Schon, E.A. (1992). Defects in mitochondrial protein synthesis and respiratory chain activity segregate with the tRNA(Leu(UUR)) mutation associated with mitochondrial myopathy, encephalopathy, lactic acidosis, and strokelike episodes. Mol. Cell. Biol. *12*, 480–490.

27. Rossmanith, W., and Karwan, R.M. (1998). Impairment of tRNA processing by point mutations in mitochondrial tRNA(Leu)(UUR) associated with mitochondrial diseases. FEBS Lett. *433*, 269–274.

28. Tomari, Y., Hino, N., Nagaike, T., Suzuki, T., and Ueda, T. (2003). Decreased CCA-addition in human mitochondrial tRNAs bearing a pathogenic A4317G or A10044G mutation. J. Biol. Chem. *278*, 16828–16833.

29. Christian, B.E., and Spremulli, L.L. (2010). Preferential selection of the 5′-terminal start codon on leaderless mRNAs by mammalian mitochondrial ribosomes. J. Biol. Chem. *285*, 28379–28386.